ADVANCED OPTICAL MATERIALS
www.advopticalmat.de

Wavelength and Stacking Order Dependent Exciton Dynamics in Bulk ReS_2

*Yongjian Zhou and Yaguo Wang**

Exciton dynamics in ReS_2 are rich and complicated due to its unique lattice and band structures. With femtosecond pump-probe spectroscopy, the wavelength-dependent exciton dynamics in bulk ReS_2 are studied at room temperature, and the effects from polarization and stacking order are also considered. Signatures from both bright and dark excitons are observed, where the lifetime at bright exciton levels is only several picoseconds, while it is about tens of picoseconds at dark exciton levels. The extremely long up-/down-going trend at selective wavelengths is attributed to the transition between different dark exciton levels. Two types of coherent dynamics are observed when the laser wavelength is scanned through different exciton levels: coherent optical stark effect and exciton-exciton coherent interaction, both occurring within the laser pulse width. Exciton dynamics show a similar trend for the sample with AA stacking order, regardless of polarization. For AB stacking, dark excitons for Exciton II and III are missing when probe pulse polarization is perpendicular to *b*-axis, which is attributed to the polarization and stacking-order dependent band structure. Studying the rich exciton dynamics in bulk ReS_2 at room temperature not only has scientific significance, but also facilitates the development of high-performance excitonic devices.

1. Introduction

Among the family of 2D transition metal dichalcogenides (TMDs), ReS_2 has drawn much attention due to its unique anisotropic optical,[1] thermal,[2] and electronic properties.[3,4] ReS_2 possesses a distorted 1T triclinic crystal structure. A zigzag Re chain is formed parallel along the *b*-axis through interactions of additional *d* valence electrons. As a result, the symmetry of ReS_2 is greatly reduced. It was also found that ReS_2 has two distinct stacking orders (AA & AB) that can persist to a thickness of several micrometers.[5] All these factors contribute to the rich exciton physics observed in ReS_2.[6–11]

The exciton dynamics in ReS_2 have been investigated vigorously in the past decade. Here is a summary of the main findings: i) From previous calculations, the valence band maximum (VBM) of ReS_2 is flat and difficult to determine, which makes it possible that VBM and CBM (conduction band minimum) are at different k points and hence ReS_2 might be an indirect bandgap material.[12] However, the k-difference of VBM and CBM is so small that there is still a strong peak shown in photoluminescence (PL) spectra even in bulk ReS_2 at room temperature (around 1.4 eV), corresponding to the indirect band transition.[1] This is drastically different from other TMDs, for which the monolayer has a direct bandgap with a clearly defined and strong PL peak, while bulk has an indirect bandgap with PL peak diminished. That is why there was a debate about whether ReS_2 has a direct or indirect band gap in the earlier literature.[13–16] (ii) ReS_2 has multiple bright excitons located at different k points and polarized along different directions.[1] Urban et al. studied the low temperature (≈10K) PL and pointed out that the intensity of the Exc. II should vanish if the excitons are fully thermalized and follow the Boltzmann distribution since the energy difference between two excitons is much larger than k_BT.[17] Instead, the Exc. II shows a comparable PL signal as the Exc. I, indicating that the PL signal of Exc. II originates from the hot excitons, and a low-level indirect channel quickly depopulates both Exc. I and Exc. II.[17] Exciton III is a superposed state by the excited state of Exc. I & II.[5,18,19] iii) Evidence of the existence of dark excitons has been reported in the literature in few-layer ReS_2.[13,17,20] Dark excitons are non-radiative excitons. In 2D materials, some dark excitons exist because of the parallel spins of electron-hole pairs,[21] the recombination of which requires flipping of spin directions. Other dark excitons exist because the electron and hole locate at different k points, which is called momentum-dark exciton.[20] For the momentum-dark exciton, it requires the participation of large-wavevector phonons for momentum conservation and hence causes a much longer lifetime, compared with their bright counterpart. Recently, Dhara et al. observed an abnormal temperature-dependent PL signal in ReS_2 and attributed it to the momentum-dark excitons.[20] The experimental phenomena were explained well with a model that considers one dark exciton state for each exciton (Exc. I or Exc. II).[20] It is worth noting that the dark exciton energy levels are very close to the bright excitons (16 and 5 meV below Exc. I and Exc. II, respectively), and should not be confused with the indirect band transition identified previously in

Y. Zhou, Y. Wang
Department of Mechanical Engineering
The University of Texas at Austin
Austin, Texas 78712, USA
E-mail: yaguo.wang@austin.utexas.edu
The ORCID identification number(s) for the author(s) of this article can be found under https://doi.org/10.1002/adom.202201322.

DOI: 10.1002/adom.202201322

PL,[1] which lies much lower than the exciton levels (≈1.4 eV). iv) Some short-lived coherent dynamics have been reported in few-layer ReS_2.[9,22] The coherent dynamics usually involve coherent interactions between photons/excitons (optical Stark effect)[23] and excitons/excitons[,24] etc., and usually occur when pump and probe temporally overlap.[25]

In this study, we conducted wavelength-dependent ultrafast pump-probe spectroscopy to study the exciton dynamics and coherent effects in bulk ReS_2 at room temperature and consider the effects from polarization and stacking orders. Compared with other TMD peers, the interlayer coupling of ReS_2 is much weaker, making it possible to observe stable excitons (both bright and dark) in bulk ReS_2, which usually appears in other TMDs only at mono- or few-layer scale. We observed both optical stark effects and coherent exciton/exciton interactions when the laser wavelength scans through energy levels of Exc. I, II & III. Clear signatures related to dark excitons are identified, as well as transitions among different dark exciton levels. Studying the rich exciton dynamics in bulk ReS_2 at room temperature not only has scientific significance, but also facilitates developing high-performance excitonic devices.

2. Results & Discussion

The femtosecond pump-probe measurements were performed with a mode-locked Ti:Sapphire laser (Spectra-Physics, Tsunami), with 7 nm spectral linewidth (full width at half maximum, FWHM). The pulse width at the sample position was measured to be ≈300 fs. The spot sizes of the pump and probe were measured to be 13.3 and 6.7 um, respectively. The pump and probe have the same wavelength, with a spectral width ≈7 nm, which is narrow enough to separate the dynamics of three bright excitons. For all the experiments, the pump energy is kept low enough to eliminate the free carriers or plasma effects to the exciton dynamics.

The bulk ReS_2 crystal was purchased from HQ Graphene and mechanically exfoliated onto a transparent glass substrate. The stacking order of ReS_2 can be determined by Raman spectrometry.[5,26] For AA stacking, the distance between Mode I and Mode III is around 13 cm^{-1}.[5,26] For AB stacking, the distance is around 20 cm^{-1}.[5,26] The sample thickness was measured by AFM, which is 145 nm for AA stacking and 166 nm for AB stacking (Figure S1, Supporting Information). To determine the direction of the Re–Re chain, we conducted the polarized Raman spectroscopy, and the Re–Re chain lies along the direction of the maximum Raman Mode V (≈211 cm^{-1}), which was also observed to be along the cleaved edge (Figure S1, Supporting Information).[5,27]

Figure 1 shows the wavelength-dependent ultrafast dynamics for stacking AA at pump 90°/probe 0°. In the following, we will use this condition as a representative case to do the analysis. For other conditions, please refer to S6–S12. We found that the dynamics do not depend on the pump polarization, suggesting that the excited carriers redistribute within the pulse width (≈300 fs). The temporal profiles evolve with wavelength, displaying interesting short-time dynamics and long-time dynamics. When the wavelength scans through the different exciton levels, the laser can sense the contribution from different sources because of the finite widths of both excitons and the laser itself (7 nm FWHM for both pump and probe). The relative intensity depends on how close the wavelength is to the center of a specific exciton. To gain an understanding of the physics behind the wavelength-dependent data shown in Figure 1, we used the following model to fit the data[28]:

$$g_0(t) = C_0\delta(t) + u(t)\left(A_1\exp\left(-\frac{t}{\tau_1}\right) + A_2\exp\left(-\frac{t}{\tau_2}\right) + A_3\left(1-\exp\left(-\frac{t}{\tau_R}\right)\right)\right) \quad (1)$$

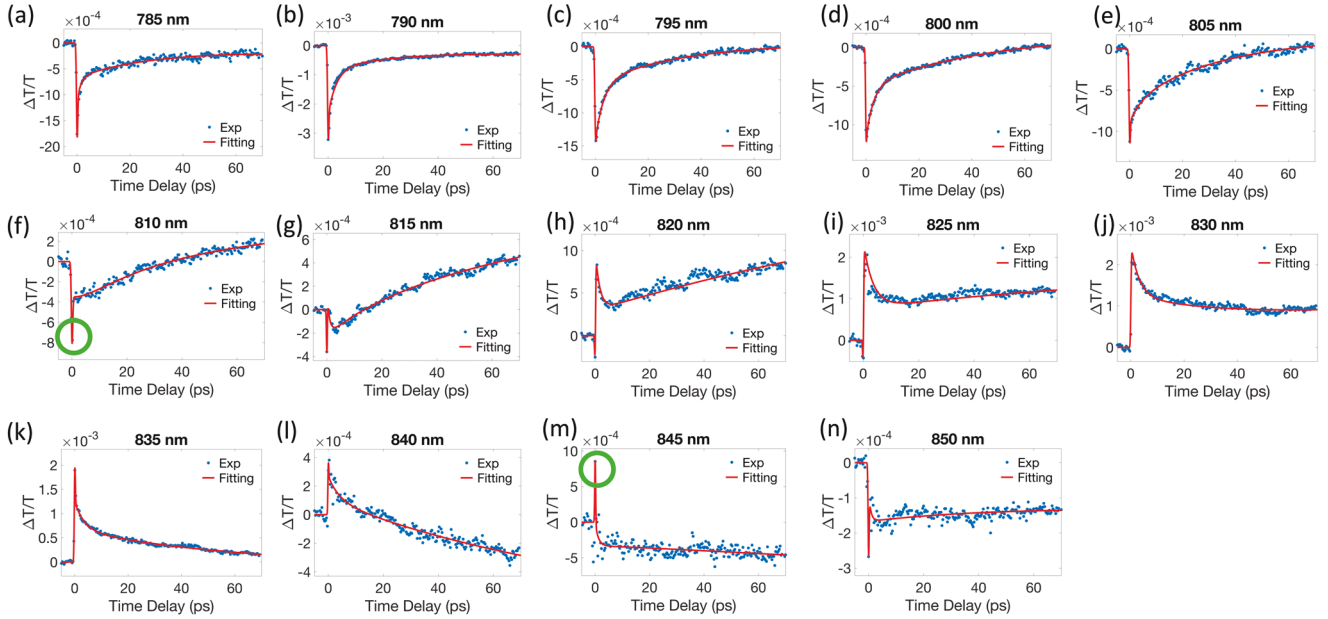

Figure 1. Wavelength-resolved degenerate pump-probe measurement for stacking AA at pump 90°/probe 0° with pump fluence at 47.18 μJ cm^{-2}. The raw data is partially adapted with permission from ref. [5] The red curves are the fitting results based on Equation 1.

$$\mathrm{IRF} = C_1 \exp\left(-\frac{t}{w^2}\right) \quad (2)$$

where $g_0(t)$ consists of dynamics from different resources, IRF is the instrument response function. $u(t)$ represents the step function. The experimental data is fitted with $g(t)$, which is the convolution of $g_0(t)$ and IRF: $g(t) = g_0(t) \otimes \mathrm{IRF}$. C_0 is related with coherent dynamics (happens within the time when pump and probe are overlapped), and the A_1 term represents the bright exciton dynamics. Both A_2 and A_3 are associated with dark excitons, where A_2 term represents the excitation and relaxation at the dark exciton levels, and A_3 represents the transition between different dark exciton levels.

Bright Excitons: To determine the bright exciton position, we conducted polarized PL measurements. The exciton positions are summarized in Table S1, Supporting Information. The shape of the polarized PL is independent of incident laser polarization, which is consistent with previous publications.[5] Based on our PL spectra of ReS_2 for different stacking orders (Figure S3, Supporting Information), the exciton levels can be determined by fitting the experimental data with the voigt function. For AA stacking, the three Exciton levels roughly sit around: Exc. III 1.565 eV (792 nm), Exc. II 1.499 eV (827 nm), and Exc. I 1.459 eV (850 nm); For AB stacking: Exc. III 1.563 eV (793 nm), Exc. II 1.521 eV (815 nm), and Exc. I 1.480 eV (838 nm).

In Equation 1, the bright exciton dynamics is represented as $A_1 \exp\left(-\frac{t}{\tau_1}\right)$. For stacking AA with pump 90°/probe 0°, the transient transmission changes related to bright excitons are plotted together in **Figure 2**a for the representative wavelengths. The peak is negative for Exciton III, but positive for Exciton II and I. The negative peak means that the absorption increases upon excitation and is associated with excited state absorption. The positive peaks are shown for Exc. I & II means absorption decreases and a related to Pauli Blocking. Pauli Blocking occurs when the exciton density of states at a certain energy level is low compared with the number of excitons generated.

Figure 2b shows the fitted lifetime (τ_1) associated with bright excitons. All the τ_1 values are around several ps, regardless of the wavelength. At the wavelength of Exc. III (790 nm), power-dependent experiments were conducted to confirm that all the measurements are in the linear region, (Figure S4, Supporting Information), and the broadening of exciton should not be important. Wang et al. did time-resolved photoluminescence and showed the lifetimes of Exc. I and Exc. II are less than 10 ps for a trilayer ReS_2 at 10 K.[13] Unlike other 2D materials, the PL width of bulk ReS_2 is only broadened a little compared to the few-layer one at the same temperature.[1] Thus, the exciton lifetime of few layers and bulk should be similar. On the other hand, the PL width broadens around 3 times larger from 10 K to room temperature.[8] Thus, we estimate that the lifetime of excitons at room temperature for bulk ReS_2 should be around a few ps, and our measured lifetime of bright excitons is consistent with the literature. The ultrafast dynamics and nonlinear optical response of Exc. III were studied previously,[5,29,30] which will not be repeated here.

Dark exciton: As proposed by Dhara et al. multiple dark excitons might exist close to the energy of bright exciton levels, as shown in their temperature-dependent PL.[20] The lifetime of the dark excitons should be much longer than the bright excitons due to the need of phonons to assist the recombination and could be around several tens of ps at room temperature.[13] The closeness of the dark excitons and bright excitons might originate from the flat band structure of ReS_2. Gehmann et al. probed the band structure of ReS_2 by k-space photoemission microscopy and found out the VBM is very flat,[12] which is also consistent with another simulation work.[13] Because the energy levels of the bright exciton and dark exciton are very close, the absorption cross-sections and exciton-exciton scattering should be similar. As revealed in the experimental data in Figure 1, at some wavelengths (e.g., 805, 815, and 840 nm), after the peaks, the spectra do not show a trend going back to the background, instead, continuous up-going or down-going trends appear and cause the signals diverge further away from the zero background. Within the time scale of our experiments, no sign of relaxation to the background was observed. Because the up-/down-going trends last for more than several tens of ps, they should not come from the bright excitons. To have a delayed up-/down- going signal, another source should exist to continuously provide the carriers to that dark exciton state after the initial excitation. These extremely long dynamics may be associated with carriers scattered from the upper-lying dark excitons to this lower-lying exciton. Mandal et al. observed a similar

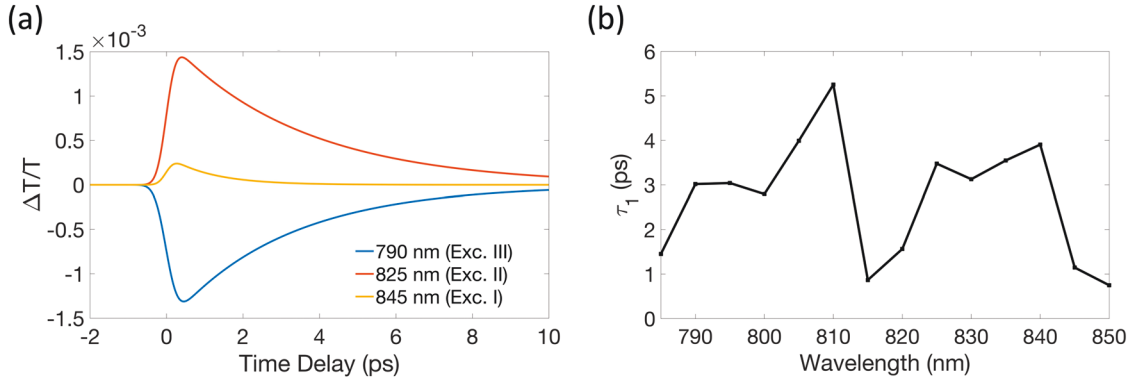

Figure 2. Bright exciton dynamics in stacking AA (pump 90°/ probe 0°). a) Decomposed signals of bright exciton dynamics at the resonant wavelengths. b) The fitted values of τ_1 at different wavelengths.

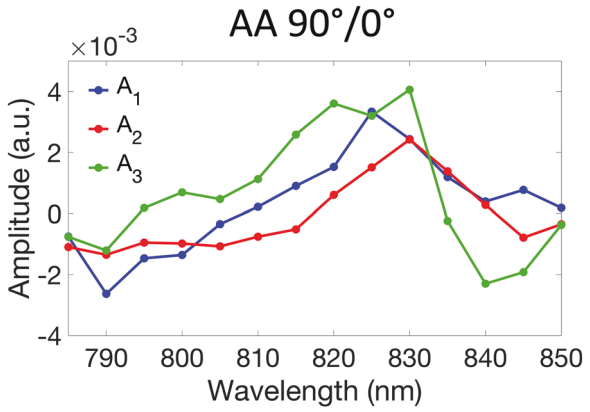

Figure 3. Comparison of the trends of A_1, A_2, and A_3 for stacking AA with pump 90°/probe 0°.

signal, and the delayed rising signal was explained as the contribution from some possible lower-lying defect states.[31] The defect states usually lie well below the CBM and its effect should be similar when the laser wavelength swipes through different excitons. The up-/down-going trends show a strong dependence on the laser wavelength, which indicates that the specific phenomena should not come from defects. Also, since our sample is bulk, the impact from the surface defects should not be important.

In Equation 1, two terms are used to describe the dynamics associated with dark excitons. The first term is: $A_2 \exp\left(-\frac{t}{\tau_2}\right)$, corresponding to the exciton excitation and recombination at a certain dark exciton level. The second term is: $A_3(1-\exp\left(-\frac{t}{\tau_R}\right)$, corresponding to the scattering process from a higher dark exciton level to a lower dark exciton level (e.g., dark Exc. II to dark Exc. I). **Figure 3** shows the trend of A_1 (bright exciton), A_2 and A_3 for AA stacking with pump 90°/probe 0°. The similar wavelength-dependent trend of A_1 and A_2 indicates that the exciton and its associated dark exciton are indeed very close to each other. Noticeably, the peak of A_2 always appears near the same position as A_1 or at a wavelength 5 nm below, which suggests the dark excitons lie below the bright exciton with an energy difference of several nm. Considering the finite pulse spectrum width, this is consistent with what was proposed by Dhara et al. that the dark excitons are just a couple of mV away from the bright excitons.[20]

Around Exc. III level (≈790 nm), A_3 remains negative. With a photon energy much higher than the dark Exc. II, the probe is most likely absorbed by the scattered carriers on the dark Exc. II. With increasing wavelength, A_3 gradually becomes positive. When it is closer to the dark Exc. II, the Pauli blocking of the carriers scattered onto the dark Exc. II becomes more dominant. Then, at an even longer wavelength, A_3 becomes negative again, sensing the dark Exc. I via excited state absorption.

Coherent effect: As shown in Figure 1 (marked with green circles), some extremely sharp peaks appear within the time scale comparable to the pump pulse width, e.g., 810 nm (negative), 845 nm (positive). There are two possible mechanisms contributing to this process. One is the coherent exciton dynamics, which reflects the exciton homogeneous broadening and the dephasing process.[24,32,33] Moody et al. studied the intrinsic homogeneous broadening in monolayer WSe_2 with four-wave mixing.[33] They found that the dephasing time is inversely proportional to both the excitation density (exciton-exciton dephasing process) and temperature (exciton-phonon interactions).[33] The extracted dephasing time at zero temperature and zero exciton density are around 400 fs.[33] With elevated temperature and finite excitation density, the dephasing time drops very fast.[33] At low excitation density, the dephasing time drops to 150 fs around 50 K.[33] Thus, the dephasing time should be at most tens of fs or even shorter at room temperature. For simplicity, in our model, a delta function is used to capture this extremely fast process. Trovatello et al. studied the coherent process in monolayer MoS_2.[24] They found that the coherent signal is much weaker when the photon energy of the pump laser is higher, due to the exciton-phonon interactions.[24] In our setup, since the pump and probe share the same wavelength and are lower than the band gap, the coherent process could be enhanced. Another possible mechanism is the optical stark effect.[9] When the optical stark effect happens, the exciton will be "pushed up" and blue shift, which should cause a decreased absorption (increased transmission) in our setup.[9] Since it responds coherently and can only happen within a pulse duration,[23] it is also represented here by a delta function.

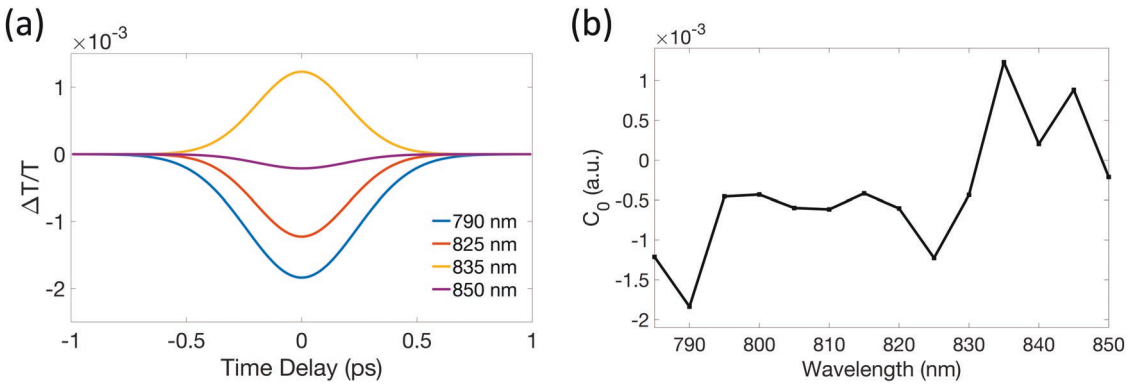

Figure 4. The coherent process is shown in stacking AA (pump 90°/ probe 0°). a) Decomposed signals of coherent process for the representative wavelengths. b) The amplitude of C_0 (coherent process).

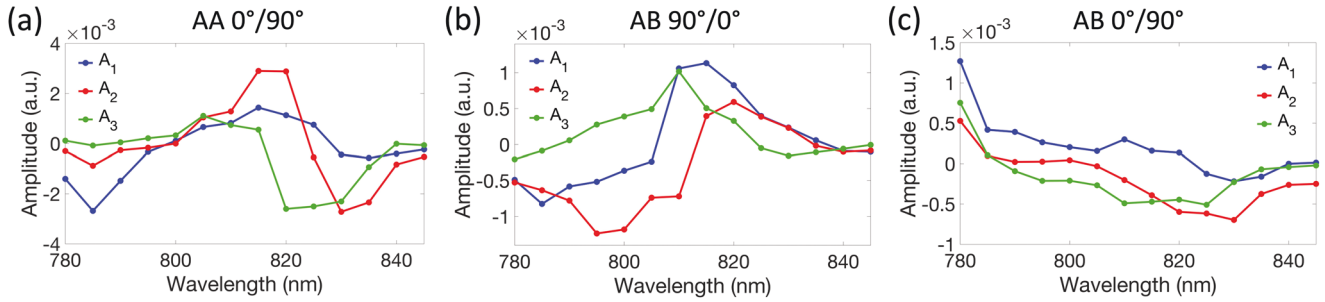

Figure 5. Comparison of the trends of A_1, A_2, and A_3 for different stacking orders with different pump/probe polarization combinations. a) AA: pump 90°/probe 0°; b) AA: pump 0°/probe 90°; c) AB: pump 90°/probe 0°; d) AB: pump 0°/probe 90°.

To make it happen, the laser photon energy usually needs to be relatively lower than the exciton.[9]

Figure 4 shows the coherent process ($C_0\delta(t)$) for stacking AA with pump 90°/probe 0°. When the wavelength is around Exc. III level (~790 nm), a sharp negative peak exists around the time zero. Since the pump and probe are at the same energy, there is no excess energy to generate phonons directly. Thus, we attribute the dephasing process at this wavelength mainly to the exciton-exciton coherent interaction. Sie et al. suggest that an attraction-repulsion crossover might exist for excitons depending on the excitation density.[34] For low exciton density, there should be an attractive force among excitons, which will produce a negative inter-exciton potential energy.[34] If that is the case, a redshift of the exciton could be observed at low density,[34] which will increase the absorption. When the wavelength is scanned to around 825 nm, another negative sharp peak shows. This wavelength corresponds to the Exc. II energy level, which is shown in PL and matches the peak in Figure 3. The origin could also be similar as the one in 790 nm. As shown in Figure 4b, when the wavelength keeps increasing, the C_0 shows a positive peak around 835 nm, which could be due to the optical stark effect.[23] Sangwan et al. observed the optical stark effect of few-layer ReS_2.[23] And they were able to control the Exc. I and Exc. II independently, which means that those two excitons are not correlated.[23] When the wavelength keeps increasing to around 850 nm (Exc. I), the C_0 becomes negative again, which could still be due to the attraction force. In the end, whether it shows positive or negative peak should depend on the relative strength of different coherent processes.[24,25]

Unlike other TMDs, ReS_2 has two distinct stacking orders, which persist to even bulk. ReS_2 also possesses anisotropic physical properties due to its unique crystal structure. Effects on the exciton dynamics from stacking order and polarization have to be considered. Figures 3 and 5 compare the A_1, A_2 & A_3 trends for different stacking orders at different polarization combinations. Case AA pump 0°/probe 90° and case AB pump 90°/probe 0° show a similar trend as case AA pump 90°/probe 0°, and the A_1 & A_2 have local maximum/minimum values near the exciton levels (bright or dark). However, for the case AB pump 0°/prob 90°, the trend is rather peculiar. As shown in **Figure 5**c, for AB pump 0°/probe 90°, both A_1 and A_2 become positive and keep increasing even at 780 nm. This trend will be discussed in the following text.

To further analyze the effects on exciton dynamics from stacking orders and polarizations, the fitted values of A_1, τ_1 (bright exciton), A_2 and τ_2 (dark exciton) for these four configurations are summarized in **Tables 1** and **2** at the three exciton levels. Since τ_R represents the scattering process from one dark exciton to another, which only plays an important role when the wavelength lies between two exciton levels. So, we leave out the A_3 and τ_R values. By comparing these fitted values, we have the following observations:

i. All the values for τ_1 are less than 10 ps, regardless of stacking order and polarization, and these values are consistent with previous research.[13]
ii. The values for τ_2 are around 50 ps (room temperature) for most of the cases, which are also consistent with previous research.[13]
iii. For stacking AA at Exc. II level, when the probe is 0°, the τ_2 is much larger than other cases. The much longer τ_2 indicates a much weaker oscillator strength, hence weaker interaction between electron-hole pairs and less tendency to recombine. Exc. II is polarized along 90° probe and hence it is reasonable to observe weaker oscillator strength along 0° probe. For AB stacking, τ_2 along 0° probe is also longer than that along 90° probe, but the difference is less dramatic. As pointed out in our previous report, the main difference between AA and AB stacking lies in the interlayer interactions.[5] For AA stacking, interlayer interaction is weaker than AB, and the behavior of

Table 1. Exciton lifetime for stacking AA.

Exciton	90°/0°				0°/90°			
	A_1	τ_1 [ps]	A_2	τ_2 [ps]	A_1	τ_1 [ps]	A_2	τ_2 [ps]
Exc. I	5.8×10^{-4}	0.95	-2.5×10^{-4}	50.98	-2.3×10^{-4}	4.68	-5.3×10^{-4}	45.49
Exc. II	3.3×10^{-3}	3.48	1.5×10^{-3}	175.57	1.6×10^{-4}	3.19	-1.6×10^{-3}	44.96
Exc. III	-2.6×10^{-3}	3.02	-1.3×10^{-3}	29.19	-8.5×10^{-4}	2.69	-2.1×10^{-4}	22.30

Table 2. Exciton lifetimes for stacking AB.

Exciton	90°/0°				0°/90°			
	A_1	τ_1 [ps]	A_2	τ_2 [ps]	A_1	τ_1 [ps]	A_2	τ_2 [ps]
Exc. I	-1.4×10^{-5}	1.92	-5.8×10^{-5}	57.90	-8×10^{-5}	3.66	-3.2×10^{-4}	37.48
Exc. II	1.1×10^{-3}	1.23	4.0×10^{-4}	73	1.6×10^{-4}	3.15	-3.9×10^{-4}	40.85
Exc. III	-5.5×10^{-4}	2.33	-9.5×10^{-4}	29.60	3.2×10^{-4}	3.36	2.4×10^{-5}	108.25

excitons is similar to that of monolayer, and hence more anisotropic than AB stacking.[5] As a result, the difference of τ_2 along 0° probe and 90° in AA stacking can be larger than that of AB stacking.

iv. For stacking AB at Exc. III level, when the probe is along 90°, τ_2 is much larger than other cases. As shown in Figure 5c for AB 0°/90°, A_2 does not show any peak around Exc. III level, indicating that there might not be well-defined dark exciton state for AB Exc. III at K1 point (probe 90°). So, this τ_2 may correspond to other processes. Mandal et. al. measured non-polarized absorption spectra of stacking AB and showed that the energy of Exc. III (≈1.56 eV) is very close to the conduction band minimum.[31] Carriers on Exc. III could be excited to the conduction band via thermal activation. These carriers later would fall back to Exc. III and recombine, which can result in a much longer lifetime. Thus, τ_2 here mostly represents the increased lifetime of the bright exciton due to the strong exciton-phonon scattering at K1 point. For other cases, the lifetimes are all ≈20–30 ps, indicating a relatively fast nonradiative process at room temperature. The peculiar trend observed in Figure 5c could also be understood in the same way, which might originate from the enhanced Pauli blocking at the bottom of the conduction band. Due to the thermal ionization of excitons from bright Exc. III to the conduction continuum, what we measured could actually be the screening from the free carriers on the conduction band, which also explain why there is a sudden big jump (closer to the conduction continuum) around 785 nm.

Now we want to explain why the dark Exc. III may not exist for AB pump 0°/probe 90°. Exc. III is considered as a superposition of excited states for both Exc. I and Exc. II, hence the dark Exc. III should also consist of contributions from both dark Exc. I and dark Exc. II. For AB pump 0°/probe 90°, near Exc. I level, both A_1 and A_2 show clear peaks in Figure 5c, suggesting well-defined bright Exc. I and dark Exc. I. According to PL, the Exc. II for AB stacking is around 810 nm. Since Exc. II is polarized perpendicular to the *b*-axis, the signal should be rather strong with probe along 90°. Near Exc. II level, A_1 shows a small peak near 810 nm, while A_2 does not show any features and the magnitude is also small. This indicates that there might be no dark Exc. II perpendicular to the b-axis (probe 90°) in AB stacking. From simulations conducted by Oliva et al., Exc. I & Exc. II locate at different high symmetry points, one at Z point (Exc. I) and the other at K1 point (Exc. II).[10] At the same time, the curvatures near the CBM and VBM are different in different directions.[10] Schematics of relations between band structure and exciton transitions are plotted in **Figure 6**. While Exc. I may have indirect states along both parallel (probe 0°) and perpendicular (probe 90°) directions to the *b*-axis, Exc. II could only have indirect states along the parallel direction but not along the perpendicular direction. Another simulation work conducted by Wang et al. suggests that the band structure could shift between direct/indirect bands when stacking order changes.[13] Based on this, we propose that for stacking AA, both Exc. I and Exc. II have indirect states along parallel and perpendicular directions to *b*-axis; for stacking AB, Exc. I has a similar situation to that of stacking AA, but Exc. II only has an indirect state along parallel direction, but not along perpendicular direction to *b*-axis. This could explain why Exc. III does not have a well-defined indirect state for AB pump 0°/probe 90°.

3. Conclusion

In summary, we measured the ultrafast dynamics of different excitons along different polarizations and identified multiple processes for ReS_2 with different stacking orders. The extremely

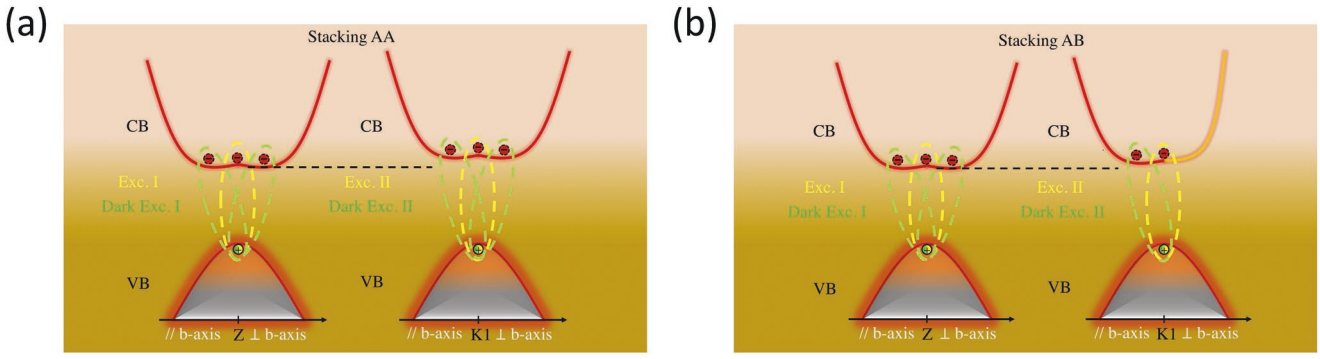

Figure 6. Schematic to illustrate the possible band structures along different directions for a) stacking AA and b) stacking AB.

sharp peak around time zero was attributed to the coherent processes. The delayed rising signal was attributed to the scattering process from high-lying dark excitons to the lower-lying dark excitons, which also evidences the existence of multiple dark exciton states. The different dynamics for stacking AB with pump 0°/ probe 90° might originate from a missing of indirect state perpendicular to the b-axis.

Supporting Information

Supporting Information is available from the Wiley Online Library or from the author.

Acknowledgements

The authors were grateful for the support from the National Science Foundation (NASCENT, Grant No. EEC-1160494 and Center for Dynamics and Control of Materials DMR-1720595; CBET-2211660).

Conflict of Interest

The authors declare no conflict of interest.

Data Availability Statement

The data that support the findings of this study are available from the corresponding author upon reasonable request.

Keywords

exciton dynamics, polarization, stacking order, transition metal dichalcogenides

Received: June 8, 2022
Revised: August 9, 2022
Published online: September 9, 2022

[1] O. B. Aslan, D. A. Chenet, A. M. van der Zande, J. C. Hone, T. F. Heinz, *ACS Photonics* **2016**, *3*, 96.
[2] H. Jang, C. R. Ryder, J. D. Wood, M. C. Hersam, D. G. Cahill, *Adv. Mater.* **2017**, *29*, 1700650.
[3] S. Yu, H. Zhu, K. Eshun, C. Shi, M. Zeng, Q. Li, *Appl. Phys. Lett.* **2016**, *108*, 191901.
[4] C. An, Z. Xu, W. Shen, R. Zhang, Z. Sun, S. Tang, Y.-F. Xiao, D. Zhang, D. Sun, X. Hu, C. Hu, L. Yang, J. Liu, *ACS Nano* **2019**, *13*, 3310.
[5] Y. Zhou, N. Maity, A. Rai, R. Juneja, X. Meng, A. Roy, Y. Zhang, X. Xu, J. F. Lin, S. K. Banerjee, *Adv. Mater.* **2020**, *32*, 1908311.
[6] Y. Song, S. Hu, M.-L. Lin, X. Gan, P.-H. Tan, J. Zhao, *ACS Photonics* **2018**.
[7] K. P. Dhakal, H. Kim, S. Lee, Y. Kim, J. Lee, J.-H. Ahn, *Light: Sci. Appl.* **2018**, *7*, 98.
[8] S. Sim, H.-S. Shin, D. Lee, J. Lee, M. Cha, K. Lee, H. Choi, *Phys. Rev. B* **2021**, *103*, 014309.
[9] S. Sim, D. Lee, M. Noh, S. Cha, C. H. Soh, J. H. Sung, M.-H. Jo, H. Choi, *Nat. Commun.* **2016**, *7*, 13569.
[10] R. Oliva, M. Laurien, F. Dybala, J. Kopaczek, Y. Qin, S. Tongay, O. Rubel, R. Kudrawiec, *npj 2D Mater. Appl.* **2019**, *3*, 20.
[11] B. S. Kim, W. Kyung, J. Denlinger, C. Kim, S. Park, *Sci. Rep.* **2019**, *9*, 2730.
[12] M. Gehlmann, I. Aguilera, G. Bihlmayer, S. Nemšák, P. Nagler, P. Gospodarič, G. Zamborlini, M. Eschbach, V. Feyer, F. Kronast, E. Młyńczak, T. Korn, L. Plucinski, C. Schüller, S. Blügel, C. M. Schneider, *Nano Lett.* **2017**, *17*, 5187.
[13] X. Wang, K. Shinokita, H. E. Lim, N. B. Mohamed, Y. Miyauchi, N. T. Cuong, S. Okada, K. Matsuda, *Adv. Funct. Mater.* **2019**, *29*, 1806169.
[14] J. Jadczak, J. Kutrowska-Girzycka, T. Smoleński, P. Kossacki, Y. Huang, L. Bryja, *Sci. Rep.* **2019**, *9*, 1578.
[15] J. Echeverry, I. Gerber, *Phys. Rev. B* **2018**, *97*, 075123.
[16] E. Liu, Y. Fu, Y. Wang, Y. Feng, H. Liu, X. Wan, W. Zhou, B. Wang, L. Shao, C.-H. Ho, *Nat. Commun.* **2015**, *6*, 6991.
[17] J. Urban, M. Baranowski, A. Kuc, A. Surrente, Y. Ma, D. Włodarczyk, A. Suchocki, D. Ovchinnikov, T. Heine, D. Maude, *2D Mater.* **2018**, *6*, 015012.
[18] C. H. Ho, P. C. Yen, Y. S. Huang, K. K. Tiong, *Phys. Rev. B* **2002**, *66*, 245207.
[19] C.-H. Ho, Z.-Z. Liu, *Nano Energy* **2019**, *56*, 641.
[20] A. Dhara, D. Chakrabarty, P. Das, A. K. Pattanayak, S. Paul, S. Mukherjee, S. Dhara, *Phys. Rev. B* **2020**, *102*, 161404.
[21] C. Robert, B. Han, P. Kapuscinski, A. Delhomme, C. Faugeras, T. Amand, M. R. Molas, M. Bartos, K. Watanabe, T. Taniguchi, B. Urbaszek, M. Potemski, X. Marie, *Nat. Commun.* **2020**, *11*, 4037.
[22] S. Sim, D. Lee, A. V. Trifonov, T. Kim, S. Cha, J. H. Sung, S. Cho, W. Shim, M.-H. Jo, H. Choi, *Nat. Commun.* **2018**, *9*, 1.
[23] S. Sim, D. Lee, J. Lee, H. Bae, M. Noh, S. Cha, M.-H. Jo, K. Lee, H. Choi, *Nano Lett.* **2019**, *19*, 7464.
[24] C. Trovatello, F. Katsch, N. J. Borys, M. Selig, K. Yao, R. Borrego-Varillas, F. Scotognella, I. Kriegel, A. Yan, A. Zettl, *Nat. Commun.* **2020**, *11*, 5277.
[25] F. Katsch, M. Selig, A. Knorr, *2D Mater.* **2019**, *7*, 015021.
[26] X.-F. Qiao, J.-B. Wu, L. Zhou, J. Qiao, W. Shi, T. Chen, X. Zhang, J. Zhang, W. Ji, P.-H. Tan, *Nanoscale* **2016**, *8*, 8324.
[27] D. A. Chenet, O. B. Aslan, P. Y. Huang, C. Fan, A. M. van der Zande, T. F. Heinz, J. C. Hone, *Nano Lett.* **2015**, *15*, 5667.
[28] R. P. Prasankumar, A. J. Taylor, *Optical tTechniques for Solid-State Materials Characterization*, CRC Press, Boca Raton, FL **2016**.
[29] Y. Zhou, N. Maity, J.-F. Lin, A. K. Singh, Y. Wang, *ACS Photonics* **2021**, *8*, 405.
[30] X. Meng, Y. Zhou, K. Chen, R. H. Roberts, W. Wu, J. F. Lin, R. T. Chen, X. Xu, Y. Wang, *Adv. Opt. Mater.* **2018**, *6*, 1800137.
[31] D. Mandal, M. Shrivastava, S. Sharma, A. K. Poonia, S. Marik, R. P. Singh, K. Adarsh, *ACS Appl. Nano Mater.* **2022**, *5*, 5479.
[32] G. Moody, J. Schaibley, X. Xu, *J. Opt. Soc. Am. B* **2016**, *33*, C39.
[33] G. Moody, C. Kavir Dass, K. Hao, C.-H. Chen, L.-J. Li, A. Singh, K. Tran, G. Clark, X. Xu, G. Berghäuser, *Nat. Commun.* **2015**, *6*, 8315.
[34] E. J. Sie, A. Steinhoff, C. Gies, C. H. Lui, Q. Ma, M. Rosner, G. Schönhoff, F. Jahnke, T. O. Wehling, Y.-H. Lee, *Nano Lett.* **2017**, *17*, 4210.